



Synthesis, Spectroscopic, and Biological Activity Study for New Complexes of Some Metal Ions with Schiff Bases Derived From 2-Hydroxy Naphthaldehyde with 2-amine benzhydrazide

Bushra Mohan

Department of Chemistry , College of Science for Women, University of Baghdad, Baghdad, Iraq.
boshra.mohan1205a@cs.w.uobaghdad.edu.iq

Naser Shaalan

Department of Chemistry , College of Science for Women, University of Baghdad, Baghdad, Iraq.
naserds_chem@cs.w.uobaghdad.edu.iq

Article history: Received 14 August 2022, Accepted 15 September 2022, Published in January 2023.

doi.org/10.30526/36.1.2978

Abstract

This study describes the preparation of tetradentate Schiff base derived from the condensation of 2-Hydroxy naphthaldehyde with 2-amine benzhydrazide and the synthesis of new complexes series with a good yield. The prepared ligand was characterized using a microanalysis technique, UV-visible, FT-IR, nuclear magnetic resonance $^1\text{H-NMR}$, mass spectrometry, thermal gravimetric analysis TGA, and the addition of conductivity measurement and magnetic moment of complexes. The invitro antimicrobial activity of the prepared compounds was tested against Gram-negative *Klebsiella pneumonia*, Gram-positive *Staphylococcus aureu*, and *Candida albicans* by the agar well diffusion method. The spectroscopy and measurement studies showed that the ligand coordinated with the metal ion as a tetradentate ligand via oxygen and nitrogen, forming an octahedral geometry around it. The ligand and its complexes positively affect the studied microorganisms' Gram-positive and Gram-negative strains and fungi.

Keywords: 2-Hydroxy naphthaldehyde, 2-amine benzhydrazide, Biological activity, Schiff base complexes.

1. Introduction

The chemistry of Schiff bases and their mineral complexes has become an area of interest for researchers because of their significant impact on human life and the environment. A general method for the synthesis of Schiff bases is the product of the condensation of aldehydes or ketones with primary amines and was first reported by the German scientist, Hikoschiff (1).

Schiff bases also described as an important mediator in many reactions, especially the formation of important porphyrins in the human body, the interaction that occurs between pyridoxal (vitamin B6) and amines and the resulting compound is (N-pyridoxylic) Schiff bases (2).

This vital importance of Schiff's rules has made them enter many areas of applied scientific research. Among the areas in the field of pharmaceutical chemistry, pharmaceutical industries, including antioxidants (3), antibacterials, antifungals, anticarcinogens (4,5), antivirals, and anti-tuberculosis (6,7) antibacterials, It has also entered the field of the industry including the manufacture of dyes (8) and polymer stabilizers and sensors (9). It should be noted that inorganic coordination chemistry has made a quantum leap through the synthesis of various coordination compounds, especially stable, essential, and biologically active chelating compounds (10, 11), including heterocyclic compounds (12).

They have also attracted researchers' interest in their catalytic and biological applications and are not limited to Schiff bases. The preparation of mineral complexes from Schiff bases with metal ions is the most important achievement that made it enter the industrial and medical fields (13), especially the pharmaceutical industry and the manufacture of insecticides, fungicides, and pesticides. Herbs and antioxidants. Which protect the living body from damage caused by harmful molecules called free radicals. The body produces cells in response to free radicals (14). 2-hydroxynaphthaldehyde derivatives have topped Schiff's rules for their importance, flexibility, and diversity of effectiveness of their compounds in all areas.

In this study, we present Schiff base ligand and metal complexes that were prepared from transition metal ions as well as zinc ion. Most of these compounds have biological activity that showed good results on gram-negative and gram-positive bacteria and promising efficacy in inhibiting the activity of fungi.

2. Materials and methods

2.1 Materials

All reagents and chemicals used in this study were in the analytical grade and purchased from (Sigma-Aldrich). 2-Hydroxy naphthaldehyde 99%, 2-amine benzhydrazide 97%, $\text{MnCl}_2 \cdot 2\text{H}_2\text{O}$ 99%, $\text{NiCl}_2 \cdot 6\text{H}_2\text{O}$ 99%, $\text{CuCl}_2 \cdot 2\text{H}_2\text{O}$ 99%, $\text{CoCl}_2 \cdot 6\text{H}_2\text{O}$ 99%, and ZnCl_2 98% were provided from BDH and used as received.

The FT-IR spectra of the ligand and its complexes were recorded within the range (200- 4000) cm^{-1} using a device of type (Shimadzu FTIR-Spectrometer) and using disk (KBr) for ligand and (CsI) for complexes at the University of Baghdad/ College of Science / Department of Chemistry. Measuring magnetic sensitivity by John Mathey device - England at Al-Nahrain University \ chemistry department

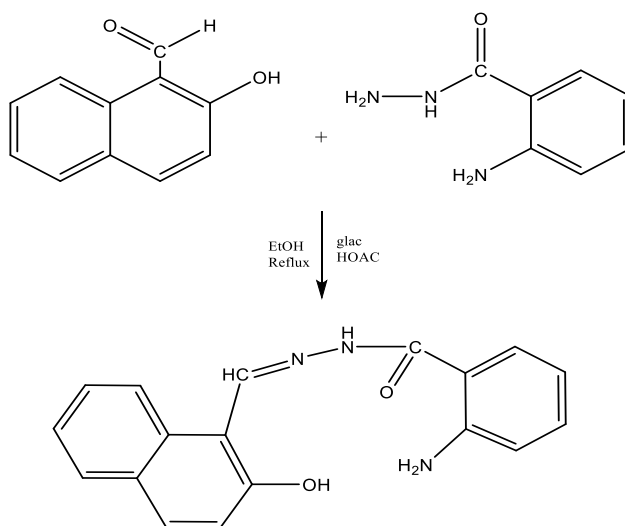
The $^1\text{H-NMR}$ spectra of the as-prepared bond were recorded using a Bruker 300MHz AVANCE spectrometer with DMSO as solvent at room temperature (Tehran). A GC-Mass-Agilent 5975c instrument recorded the mass spectra of the prepared compounds for the ligand and the compounds studied using the (Elementer Vari) instrument at Shahid Beheshti University in Tehran / Islamic Republic of Iran.

Ultraviolet Spectrophotometer A 160. The prepared solutions were at a concentration of (1×10^{-3} molar) in dimethylformamide (DMF) solvent. The melting point of the prepared ligand and its complexes were measured using an (SMP10) device from the English company Stuart in the temperature range of 300 °C. The molar conductivity was measured with a WTW meter, and the UV-visible spectra in the range (190.00-1100) nm were measured using a Shimadzu UV-Vis device.

3. Synthesis

3.1 Synthesis of the (L) ligand

A solution of 2-hydroxy-1-naphthaldehyde (0.782 gm, 0.0045 mol) in 15 ml ethanol was mixed with (0.68 gm, 0.0045 mole) 2-amine benzhydrazide in 10 ml of ethanol and three drops of glacial acetic acid were allowed to react in a 50 ml round bottom flask. The mixture was added under stirring and refluxed for 5 hrs. A yellow precipitate formed was collected by filtration, washed, and recrystallized with a mixture of hot methanol/ethanol (50:50) and then dried at 50 °C. The yield of the prepared ligand was 55%, as shown in **Scheme 1**.



Scheme 1. Synthesis L ligand

3.2. Preparation of Metal Complexes L ligand complexes

New complexes were synthesized by mixing 10 ml methanol of the metal salt (0.0018 mole) (where $M^{2+} = Mn^{2+}, Co^{2+}, Ni^{2+}, Cu^{2+},$ and Zn^{2+}) with of the ligand (0.0018 mole) (1:1) (M:L) as dissolved in 10 ml of methanol. The solution was stirred under heating at 50 °C for 2 hrs until the precipitate was formed. The colored complexes were separated by filtration, washed with methanol and ether, and left to dry at 80 °C.

Table 1. Physical data and elemental analysis of ligand and its metal complexes

Compound	molecular formula	color	M.wt g/mol	Yield (%)	C%	H%	N%	Molar Conductance Ω^{-1} Cm ⁻¹ at 26°C	Melting point (°C)
L	C ₁₈ H ₁₅ N ₃ O ₂	yellow	305.3 5	85%	70.21 (70.81)	4.626 (4.95)	13.62 (13.76)	—	190- 194
L+Mn	C ₁₈ H ₁₆ N ₃ O ₃ MnCl ₂	dark goldenrod	448	68.16	49.72 (48.42)	3.83 (3.60)	9.38 (10.71)	7.9	>300
L+Co	C ₁₈ H ₁₆ N ₃ O ₃ CoCl ₂	smith green	452	81.7	48.41 (47.81)	3.44 (3.57)	9.50 (9.29)	12.9	Dec.
L+Ni	C ₁₈ H ₁₆ N ₃ O ₃ NiCl ₂	pumpkin	452	91.9	47.67 (47.84)	3.936 (3.57)	8.552 (9.30)	67.26	>300
L+Cu	C ₁₈ H ₁₆ N ₃ O ₃ CuCl ₂	olive	457	80.21	57.77 (58.77)	3.92 (3.84)	10.54 (11.42)	11.1	Dec.
L+Zn	C ₁₈ H ₁₆ N ₃ O ₃ ZnCl ₂	yellow	459	79.17	59.31 (58.48)	3.806 (3.82)	12.14 11.37	24..2	>300

4. Results and Discussion

4.1-FT-IR Spectra

4.1.1-FT-IR Spectra of L-Ligand

The table below presents the infrared frequency bands of the Schiff base and its metal complexes. The potential binding sites through the donors are nitrogen, isomethane) (-C = N) group, a hydroxyl group (-OH), aromatic amine group-NH₂ and carbonyl group C=O. The FT-IR spectrum showed the bond synthesis method (L) in (Scheme 1). Also, the data of the ligand FT-IR spectra of the ligand showed the disappearance of (C = O) bundles of the aldehyde in the region (1683) cm⁻¹ and the amino group (-NH₂) in the region 3288-3323 cm⁻¹ and the appearance of new peaks which are the link bundles of the imine group of the prepared ligand that was in (1546) cm⁻¹. The infrared spectrum of L-free ligands showed weak broad absorption bands at 3440.77 cm⁻¹, 1093 cm⁻¹, and 2939 cm⁻¹ due to the stretching vibration of (OH), (C-O-H) and (=C-H) aldehyde (imine) respectively for L ligand.

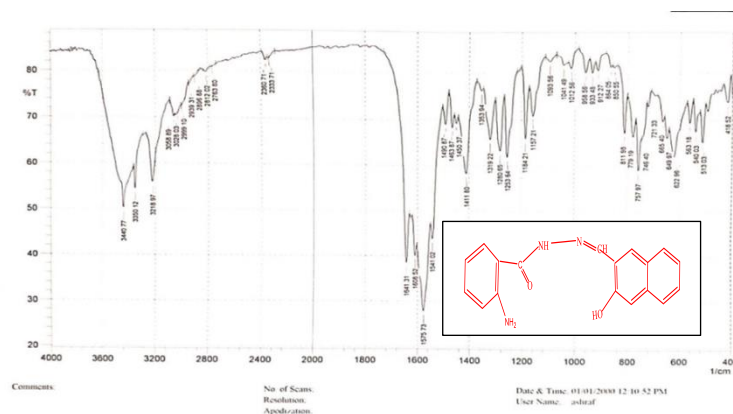


Figure 1. IR for Ligand L

4.1.2- FT-IR spectrum of the L . complexes

The comparison of the IR spectrum data of the complexes with the Free Schiff base indicates that the range of the imine group ($\text{HC} = \text{N}$) in the L complexes in L complexes has been shifted from $(1608) \text{ cm}^{-1}$ to lower frequencies in all five complexes, indicating the binding of the nitrogen atom in the group Coordination of nitrogen with a metal ion is expected to reduce the electronic density to lower frequencies in all five complexes, as the new bands of the isomethene group appeared in the region from $(1541\text{--}1546.91) \text{ cm}^{-1}$

Additionally, new weak bonds appear at $\nu (550\text{--}200) \text{ cm}^{-1}$ and are related to $\nu (\text{M-N})$, $\nu (\text{M-O})$, $\nu (\text{M-Cl})$ guide to coordination and formation of Schiff complexes. The new bands appeared in the region $(366\text{--}424) \text{ cm}^{-1}$ indicating the bonding of the nitrogen of the isomethine group with the metal, indicating the association of the nitrogen atom with the imine group ($\text{C} = \text{N}$) in coordination with the mineral (16). As shown in the tables, the disappearance of broad bands in the range $(3350\text{--}3440) \text{ cm}^{-1}$ belonging to phenol hydroxyl (O) complexes is evidence of their chelation by a phenolic oxygen atom (17). It appeared in the range $(503\text{--}592) \text{ cm}^{-1}$. A new beam due to the vibrations of the stretching group (M-O) showed the stretching group (M-N) of the as-prepared complexes in the confined region between $(366\text{--}464) \text{ cm}^{-1}$, confirming the metallicity. Cross-linking (N) atom Azomethine binding causes a shift in the ν group ($\text{CH} = \text{N}$). The absorption peak of the Schiff ligand is about 3440 cm^{-1} due to the phenolic hydroxyl group of the Schiff base ligand, and this absorption peak disappears during the process of binding with metal using metal ions. This confirms coordination through phenol ($-\text{OH}$) and the central metal ion (18).

Table 3. FT-IR data of Ligand and its metal complexes (cm⁻¹)

comp.	V(M-OH2) (OH)	V(C=N)	V(C=C)	v(C-H)	V(N-H)	V(M-Cl)	V(M-O)	V(M-N)
L	3440.77	1608	1541.02	2999	3600	----	----	----
Mn+L	3481.51	1546.91	1517.98	2871.51	37481	270 - 300 - 333	(424)	514.99
Co+L	3680	1546	1514	2883.66	3745.75	270 - 333.69	(464)	514.99
Ni+L	3369.41	1541	1541	2954	3585.42	235.30 - 258.44	(418)	555.14
Cu+L	3481.51	1546	1514	2883.58	3746.76	266.18 - 305.75	(550)	374.19(s)
Zn+L	3452.58	1546.91	1514.12	-2877.79 2819.93	3745.75	262 - 270	(424.34)	503.42- 578.64

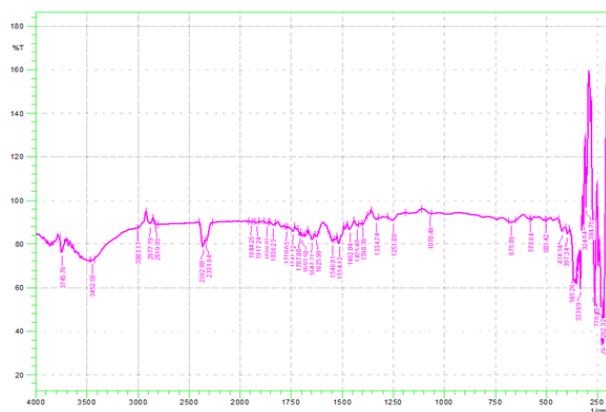


Figure 2. Zn+LComple

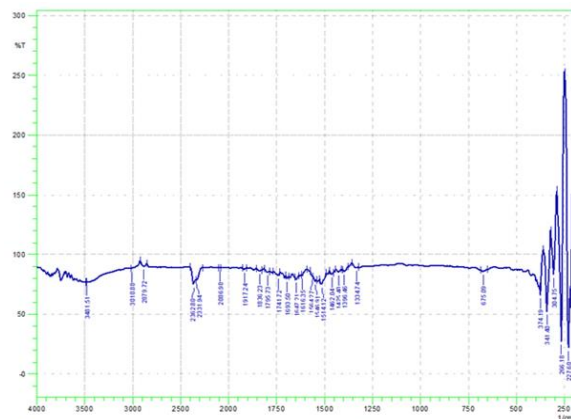


Figure 3. Cu+ Lcomple

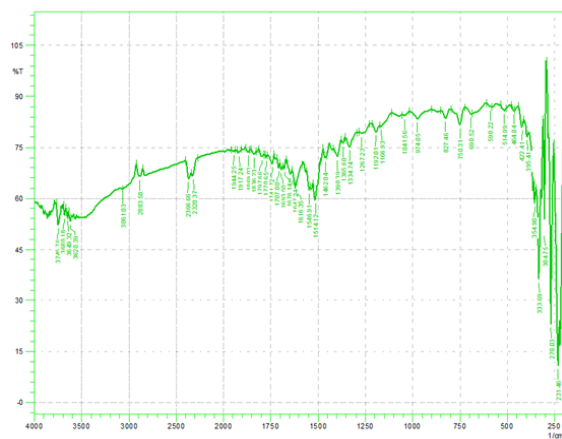


Figure 3.Co +L complex

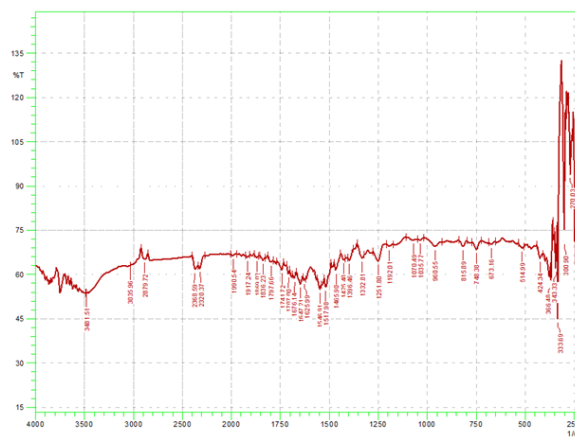


Figure 4. Mn +L complex

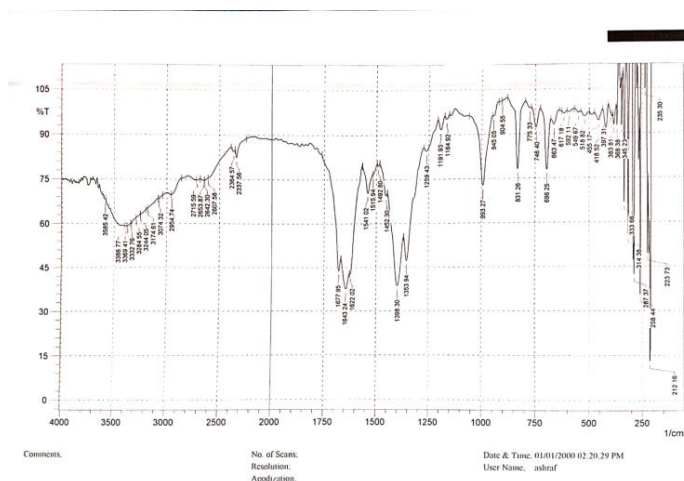
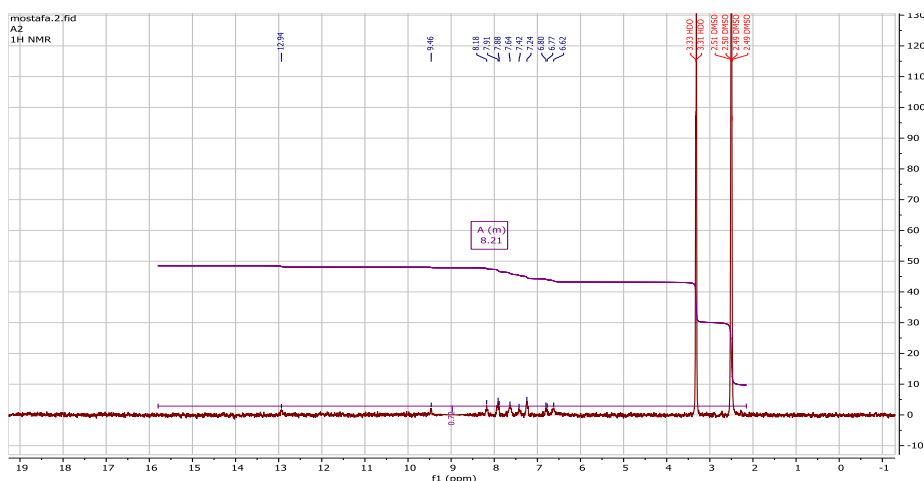
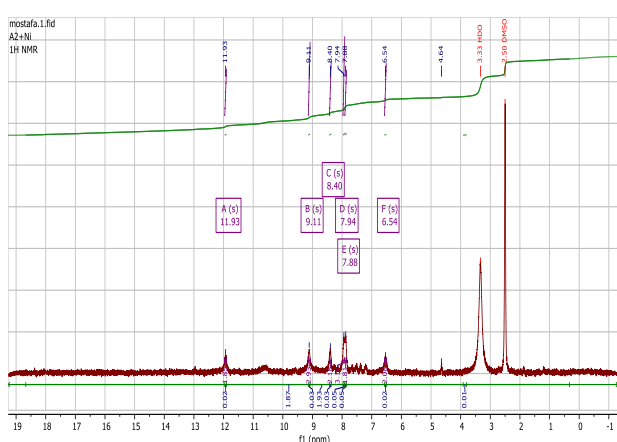
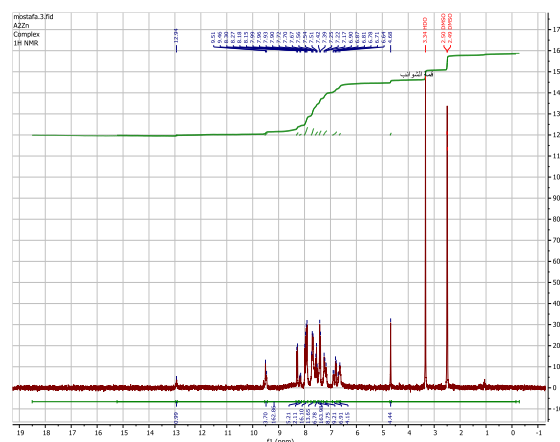


Figure 5.Ni+L complex

4.2-¹HNMR Spectrum

The Schiff base ligands and its complexes were investigated by Burker 300 MHz and using a DMSO solvent. The examined samples showed a set of traceable signals as follows: Proton analysis of the linker showed a set of signs, the first sign in the shift ($\delta = 2.49, 2.50, 2.51$ ppm) was attributed to the solvent DMSO and the next sign in the shift was two signs ($\delta = 3.32$ ppm, 3.33 ppm,) for the presence of impurities in the compounds, The tag ($\delta = 9.46$ ppm, H^+ : NH) is believed to be a proton of the NH amide group. A mark appeared after the displacement ($\delta = 8.21$ ppm, $2H^+$: NH_2) that is believed to be a proton of the NH_2 amine group attached to the benzene ring. a mark after the displacement ($\delta = 8.18$ ppm, H^+) attributed to the proton of the carbon of the isomethine group. Thet protons of two naphthaldehyde rings showed signs of displacement ($\delta = 7.24-7.91$ ppm, $10H^+$). Finally, in displacement ($\delta = 12.91$ ppm, H^+ : OH) a sign appeared that could be attributed to the proton of the hydroxyl group.

Figure 6. $^1\text{H-NMR}$ Spectrum of complexesFigure 7. $^1\text{H-NMR}$ L+NiFigure 8. $^1\text{H-NMR}$ L+Zn

4.3-Mass Spectra

The molecular weight of Schiff base L was determined using GC-Mass-Agilent 5975c technology. The mass spectra gave the compound's molecular weight identical to what was calculated theoretically ($m/e = 305$) corresponding to $(\text{C}_{18}\text{H}_{15}\text{N}_3\text{O}_2) \text{M}^+$, which is equal to 100% of the weight of the compound.

The best peak of the ion appeared at $m/e = 120$ due to $(\text{C}_7\text{H}_6\text{NO}) \text{M}^+$, equal to 39%. The best peak of the ion $m/e = 104.1$ is due to $(\text{C}_7\text{H}_5\text{CO}) \text{M}^+$, which is equivalent to 34%. Then the peak of the ion $m/e = 92$ returns to $(\text{C}_6\text{H}_4\text{O}) \text{M}^+$, which is equal to 30%, then the absorption peak $m/e = 77$ returns to $(\text{C}_5\text{HO}) \text{M}^+$, which is equal to 25%. Then, the maximum absorption $m/e = 65$ returns to $(\text{C}_4\text{HO}) \text{M}^+$. It is equal to 21% in the end. The absorption peak of $m/e = 51$ is due to $(\text{C}_3\text{O}) \text{M}^+$, which equals 16.7%.

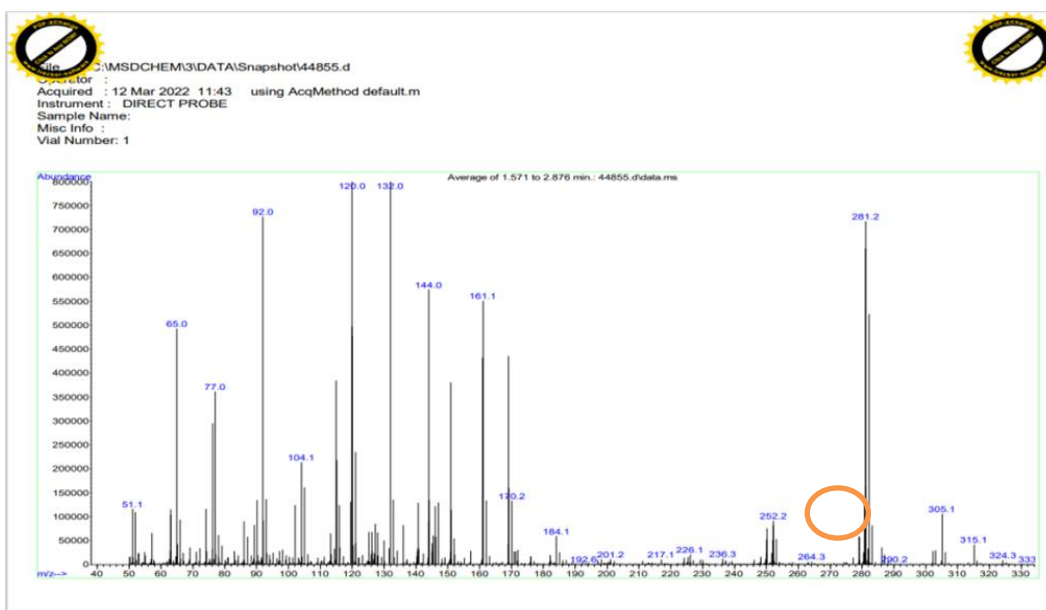


Figure 9. GC-Mass of Ligand L

4.5-UV Spectra

The electronic absorption spectra of Schiff bases and their complexes are shown in the table below. It was applied with dimethylformamide (DMF) solvent, and sample solutions were prepared at a concentration of 0.001 M.

Three bands appeared in the ligand (Schiff base) spectrum in the regions (361,320,224) nm indicating ($n \rightarrow \pi^*$), ($\pi \rightarrow \pi^*$) azomethine and hydroxy oxide group transitions, and $C = C$ aromatic bond.

The electronic spectra of the Co(II) complex showed absorption bands at (483–421) nm, the ${}^4T_{1g} \rightarrow {}^4T_{1g}(p)$ transitions. The occurrence of these transitions indicates the formation of an octahedron around the Co (II) ion. The magnetic measurements of the cobalt compound also showed a value (1.78 BM) located within the octahedral domain. The nickel complexes showed three absorption bands in the regions (944-499-443) nm, indicating that transitions occurred, respectively, ${}^3A_{2g}(F) \rightarrow {}^3T_{2g}(F)$, ${}^3A_{2g}(F) \rightarrow {}^3T_{1g}(F)$, ${}^3A_{2g}(F) \rightarrow {}^3T_{1g}(P)$. This corresponds to the octahedral composition and the magnetic moment of the nickel binary complex was (1.96 BM), and this corresponds to nickel octahedral complexes subjected to antiferromagnetic interference. As for the copper complex, three absorption bands appeared in the absorption regions (649 - 247) nm. The first band is stimulated at the transitions ${}^2B_{1g} \rightarrow {}^2A_{1g}$, ${}^2B_{1g} \rightarrow {}^2E_g$, located within the Hexagonal coordination bands, specifically octahedral. The Mn complex gave a magnetic moment value (1.67 BM) which is less than the spin of one electron. This is due to antimagnetic interference. The zinc compound is non-magnetic and does not give transitions in the visible region because its outer shell is saturated with d10. It is classified among octahedral complexes depending on the infrared spectrum. Table 4. UV-VIS data and magnetic moment value for Ligand and its metal complexes.

Table 3. UV-VIS data& magnetic moment value of Ligand and its metal complexes

NO.	Compound	color	Absorption Bands (nm)	Assigned transition	μ_{eff} (BM)	Suggested Structure
1-	L Ligand (C ₁₈ H ₁₆ N ₃ O ₂)	yellow	361 224	n→π* → C=N π→π*, →aromatic ring	-----	-----
2-	[CoLCl ₂]H ₂ O	smith green	483 421 337	4T _{1g} →4T _{1g} (p) Charge transfer	1.78	Oct.
3-	[NiLCl ₂]H ₂ O	pumpkin	944 499 443	3A _{2g} (F) → 3T _{2g} (F) 3A _{2g} (F) → 3T _{1g} (F) 3A _{2g} (F) → 3T _{1g} (P)	1.96	Oct.
4-	[CuLCl ₂]H ₂ O	olive	649 440 247	2B _{1g} → 2A _{1g} 2B _{1g} → 2E _g Charge transfer	1.84	Oct.
5-	[MnLCl ₂]H ₂ O	dark goldenrod	446 423	Charge transfer	1.67	Oct.
6-	[ZnLCl ₂]H ₂ O	yellow	534 363 216			

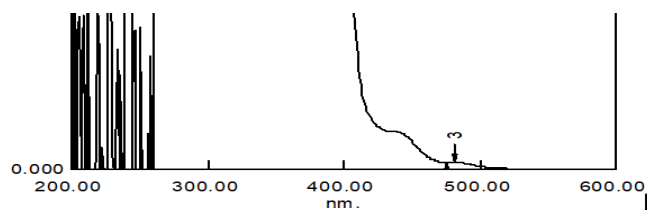


Figure 10. L Ligand UV-Spectra

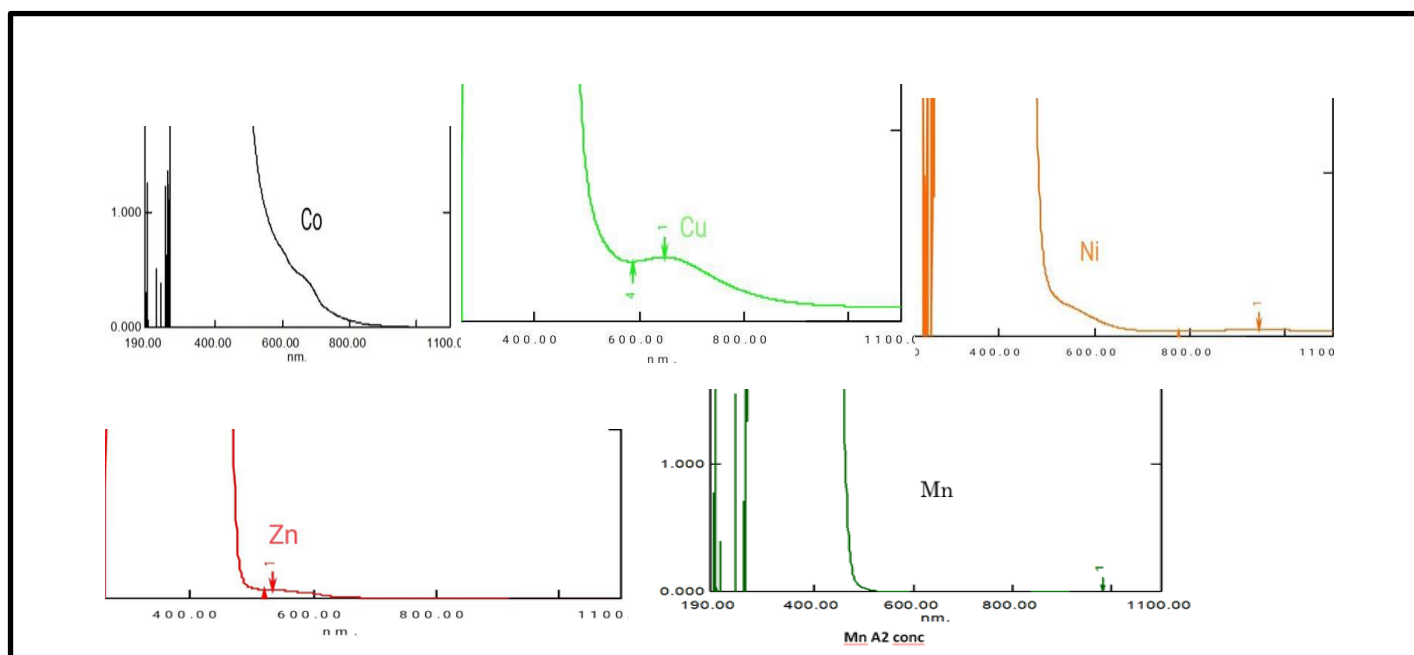


Figure 11. UV-Spectra of complexes

4.6-Thermogravimetric analysis

Thermogravimetric analysis: The reaction was carried out At (0.0 - 900) °C at about ten (10) degrees per minute. Thermal weight loss (TGA) and differential thermogravimetric analysis (DTG) in an atmosphere of air showed that (TGA), the curve of the ligand and its metal compounds was correct going through several stages of weight loss. It started with the exit of water and volatiles. The weight loss of the nickel (II) compound was analyzed in the following stages. The first stage got at (48-95) degrees Celsius, and it seemed to lose water outside the consistency ball. The percentage of weight lost was calculated (3.9%) and compared with that found (4%). In the second phase of weight loss, it is estimated that it started at (335-510) degrees Celsius, and the bulk of the weight has been lost. It was calculated as 63.7%, and it was actually found to be 63%. In the last stage, metal oxide residue (NiO) was found, and its calculated percentage equals (17%), and it was actually found equal to (18%). The zinc (II) compound was analyzed in stages: In the first stage: a period ranging (from 75-150) °C, the water loss outside the consistency ball with chlorine was consistent with the metal The loss of water outside the consistency ball with chlorine was consistent with the mineral. The weight loss was calculated and was equal to 18% of the complex weight, while it was found equal to (19.4%). In the second stage of decomposition, it was estimated that it occurred in the period (330-410) C°, and it was found that the lost weight of the compound was 20%. The calculated percentage coincided with the real one. The third stage of decomposition was estimated to occur in the period (410-640) C°. The weight lost was calculated at 43.3%, while it was actually found equal to 46%. The increase in weight was explained by interactions with the atmosphere (air), such as oxidation, because the atmosphere in which the reaction occurred was not inert. Finally, it was found that the metal oxide remained, and it was calculated at 17.3%. Its actual presence was 16%. The table below shows the stages of pyrolysis.

Table 5. Summarizes the pyrolysis processes of compounds

Sample (step)	Tem .range °C	TG Weight mass loss		Reaction	NOTE
		Calc%	found%		
L (I)	70-98	10	10.3	N ₂ H	
L (II)	200-240	34.05	33.7	C ₇ H ₄ O	
L III	240-590	39.299	40	C ₇ H ₆ NO	
LIV	590-800	9.169	9.1	C ₂ H ₄	
Final residual		7.5	6.9	C ₂	
L+Ni	48-95	3.9	4	H ₂ O	
		15.4	15	Cl ₂	
	335-510	63.7	63	C ₁₈ H ₁₄ N ₃ O	
Final residual		17	18	NiO	
L+Zn	75-150	19.4	18	H ₂ O+ Cl ₂	
	330-410	20	20	C ₆ H ₆ N	
	410-640	43.3	46	C ₁₂ H ₈ N ₂ O	The increase in weight explains that the missing part was subjected to an oxidation process
Final residual		17.3	16	ZnO	

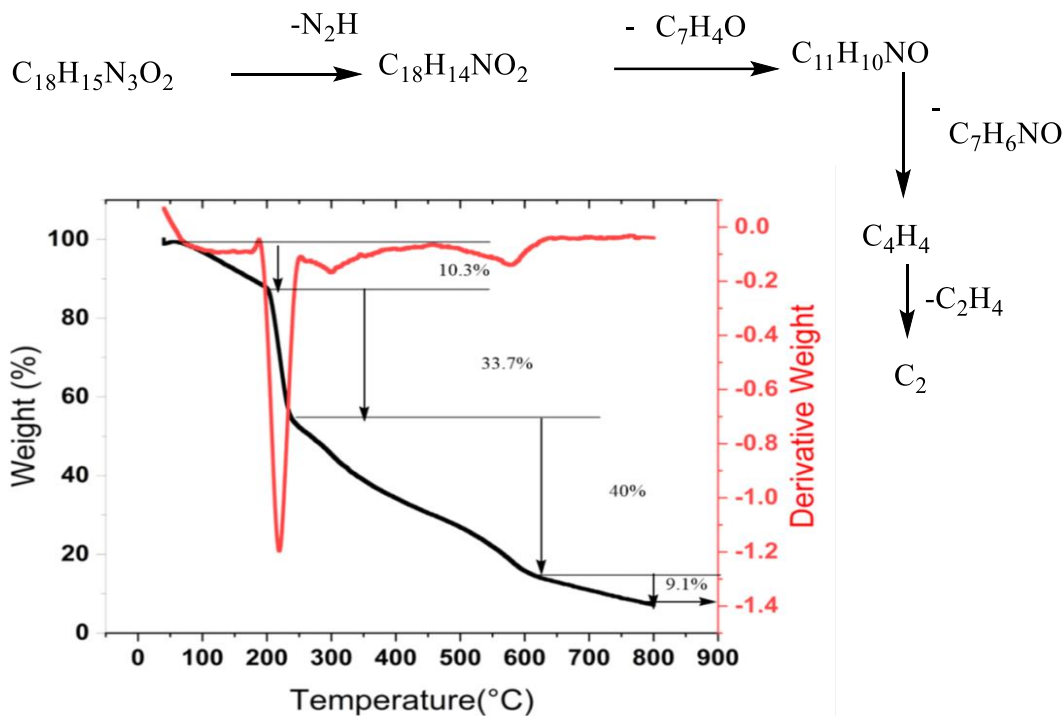


Figure 12. weight loss chart in Lligand

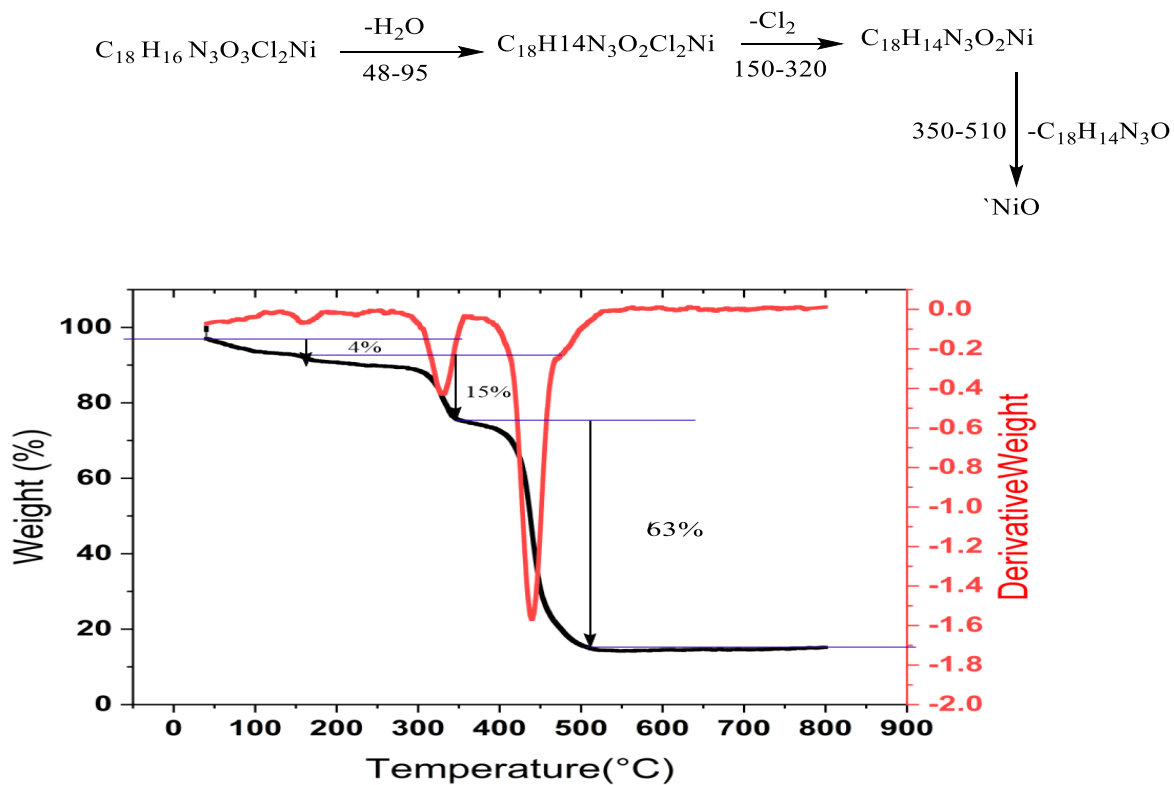


Figure 13. weight loss chart in Ni complexes

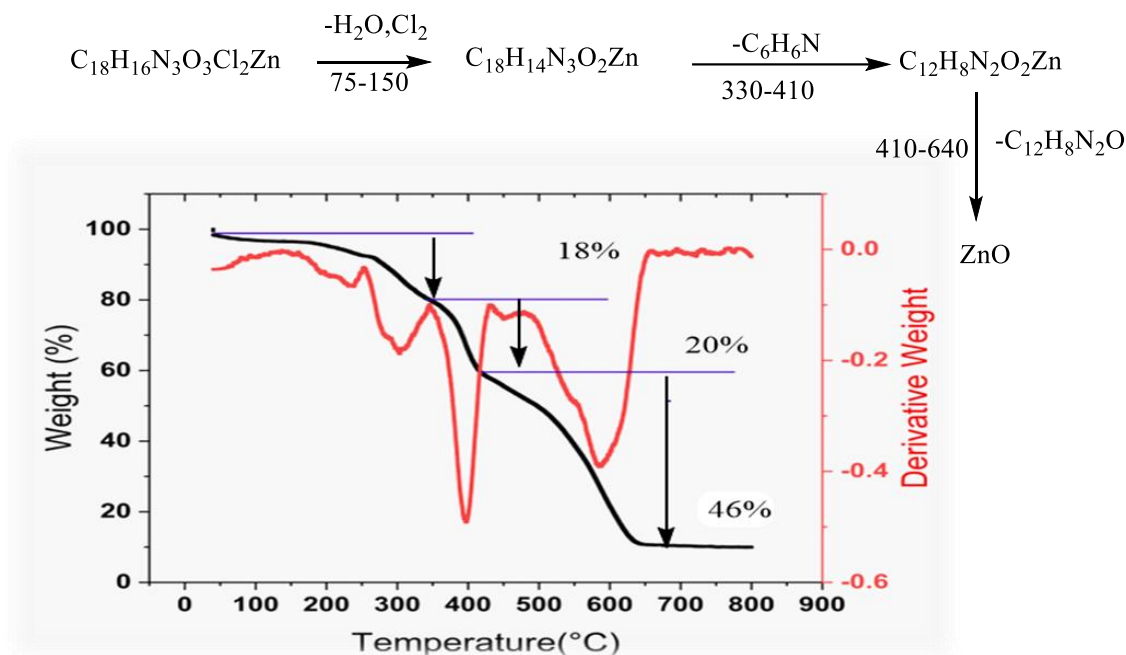


Figure 14. weight loss chart in Zn complexes

4.7-Biological Activity

The biological activity data are shown in **Table 6** and **Figure 13 and 14**. Data for the Schiff base ligand (L) and its metal complexes are presented in Table 6 below. They were tested and evaluated for their antibacterial and antifungal activity by etch-diffusion technique. The solution of the compounds was prepared in a DMF solvent at a concentration of 0.01 M (mol). Two types of pathogenic bacteria were selected under aerobic conditions at (37°C) for 24 hours, Gram-negative *Klebsiella pneumonia*, Gram-positive *Staphylococcus aureu*, and *Candida albicans*. Bacteria and fungi were preserved in nutrients, and the test showed positive results for Schiff's base and L mineral complexes, where the copper complex was No. 2. Zinc was the most active against gram-positive bacteria, while cobalt complexes No. 7 and copper No. 4 were the most active against gram-negative bacteria. Copper was most effective on *Candida albicans*, followed by nickel.

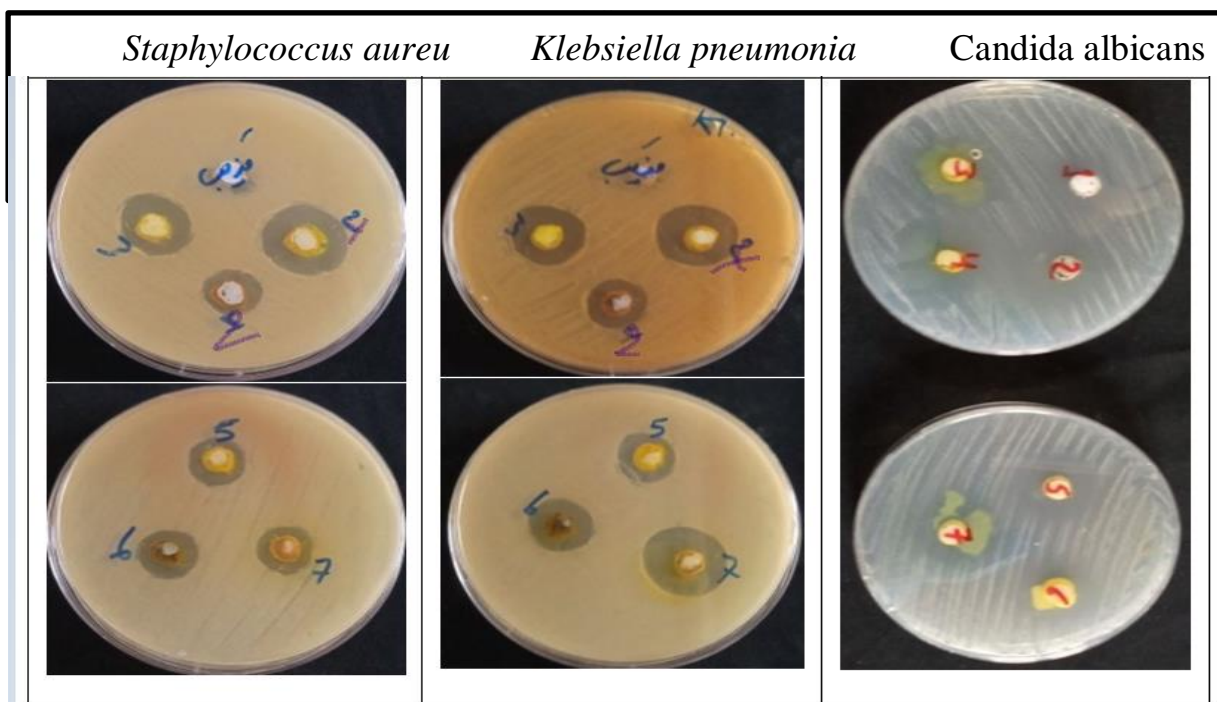


Figure 15. Biological activity of L ligand and its complexes

Table 6. The antibacterial activity of the prepared compounds

NO.	compounds	<i>Staphylococcus aureus</i>	<i>Klebsiella pneumoniae</i>	NO.	compounds	<i>Candida albicans</i>
1	Solvent DMF	negative	negative	1	Solvent DMF	20
2	Ligand A2	15	16	2	Ligand A2	22
4	[Mn(A2)Cl ₂].H ₂ O	15	16	6	[Mn(A2)Cl ₂].H ₂ O	23
7	[Co(A2)Cl ₂].H ₂ O	16	23	3	[Co(A2)Cl ₂].H ₂ O	22
5	[Ni(A2)Cl ₂].H ₂ O	17	17	7	[Ni(A2)Cl ₂].H ₂ O	24
4	[Cu(A2)Cl ₂].H ₂ O	23	23	4	[Cu(A2)Cl ₂].H ₂ O	26
3	[Zn(A2)Cl ₂].H ₂ O	20	20	5	[Zn(A2)Cl ₂].H ₂ O	22
	standard	4.32 ^a	4.32 ^a			20.41 ^b

MIC minimum inhibitory concentration(10^{-2} M)

Ofoxacin^a (C₁₈H₂₀N₃O₄)

Fluconazole^b (C₁₃H₁₂F₂N₆O)

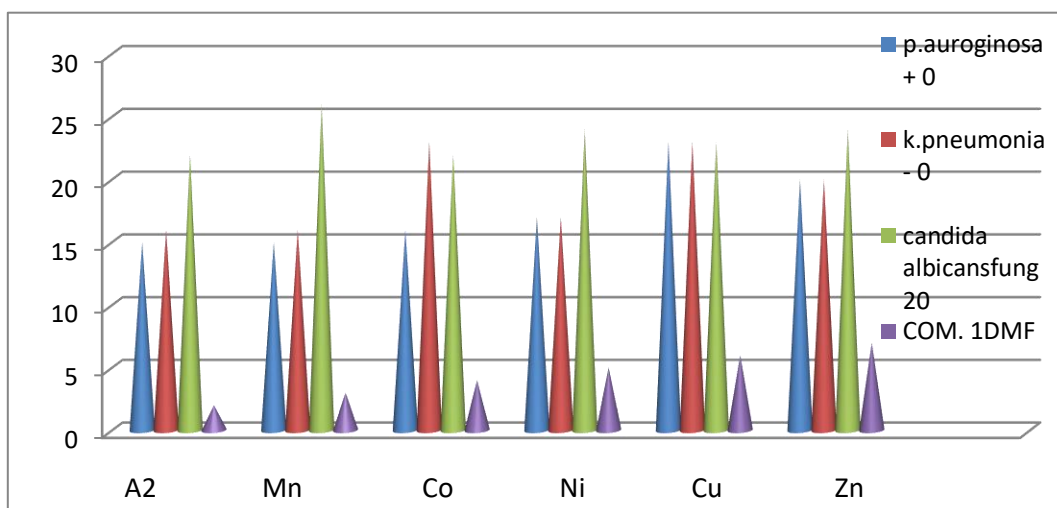


Figure 16. Antibacterial activity of ligand and their complexes

5. Conclusion

According to the previous study, the ligand was prepared by the traditional reverse reaction method. It was found that it combined with metal ions in a chelating manner. This was demonstrated by the above analyses, including infrared spectrometry that showed bonds, ultraviolet analysis, mass spectrometry analysis, gravitational and thermal analyses, etc.

The study of the biological activity of the ligand and the complexes also proved that all the prepared compounds can be described as biologically active against microbes.

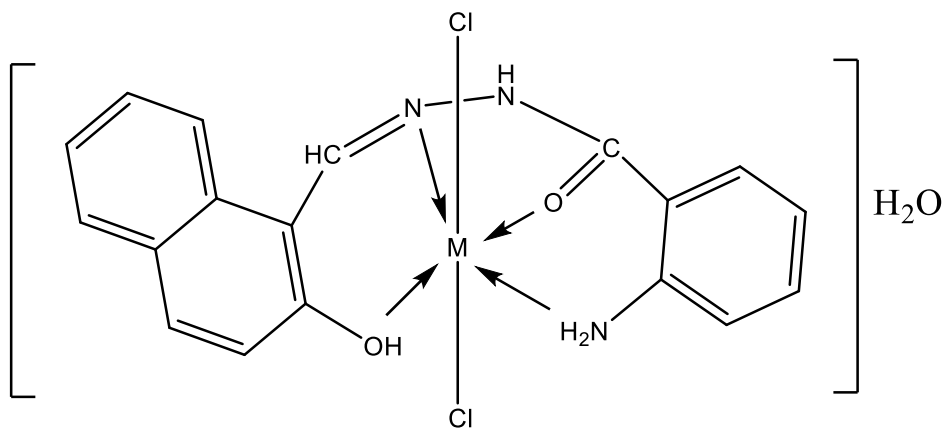


Figure 17. Suggested structure for complexes (Mn, Co, Ni, Cu, Zn)

References

1. El-Boraey, H.A.; El-Gammal, O.A.; Abdel Sattar, N.G. Impact of Gamma-Ray Irradiation on Some Aryl-Amide-Bridged Schiff-Base Complexes: Spectral, TGA, XRD, and Antioxidant Properties. *J. Radioanal. Nucl. Chem.* **2020**, *323*, 241–252.
2. El-Sonbatil, A.Z., et al. Synthesis, Characterization of Schiff Base Metal Complexes and Their Biological Investigation **2019**, 1–16.

3. Helal, T.A.; Mohammed, H.J.; Mohsein, H.F. Synthesis with Spectral Investigation of New Azomethine – Azo Ligands Derived from 4-Amino Antipyrine with Its Some Complexes. *Int. J. Pharm. Res.* **2018**, *10*, 385–390, doi:10.31838/ijpr/2018.10.03.026.
4. John, S.F.; Aniemeke, E.; Ha, N.P.; Chong, C.R.; Gu, P.; Zhou, J.; Zhang, Y.; Graviss, E.A.; Liu, J.O.; Olaleye, O.A. Characterization of 2-Hydroxy-1-Naphthaldehyde Isonicotinoyl Hydrazone as a Novel Inhibitor of Methionine Aminopeptidases from Mycobacterium Tuberculosis. *Tuberculosis* **2016**, *101*, S73–S77.
5. Maher, K. Schiff Bases Derived from 2-Hydroxynaphthalene-1-Carbaldehyde and Their Metal Complexes. *Asian J. Chem.* **2018**, *30*, 1171–1182, doi:10.14233/ajchem.2018.21286.
6. Mbugua, S., et al. New Palladium(II) and Platinum(II) Complexes Based on Pyrrole Schiff Bases: Synthesis, Characterization, X-Ray Structure, and Anticancer Activity. *ACS OMEGA* **2020**, 1–14.
7. Kumaravel, G. Utthra, P., And Raman *, N. Exploiting the Biological Efficacy of Benzimidazole Based Schiff Base Complexes with L-Histidine as a Co-Ligand: Combined Molecular Docking, DNA Interaction, Antimicrobial and Cytotoxic Studies. *Bioorganic Chem. J.* **2018**, *77*, 269–279.
8. MM, A. Green Synthesis, Spectral, Thermal Characterization and Biological Activity of Schiff Base Ligand Derived from 3-Amino-1,2,4-Triazol and Its Metal Complexes. *Org. Med. Chem. Int. J.* **2019**, *8*, doi:10.19080/omcij.2019.08.555736.
9. Neelofar; Ali, N.; Khan, A.; Amir, S.; Khan, N.A.; Bilal, M. Synthesis of Schiff Bases Derived from 2-Hydroxy-1-Naphth-Aldehyde and Their TIN(II) Complexes for Antimicrobial and Antioxidant Activities. *Bull. Chem. Soc. Ethiop.* **2017**, *31*, 445–456.
10. Orlova, N.; Nikolajeva, I.; Pučkina, A.; Belyakov, S.; Kirilova, E. Heterocyclic Schiff Bases of 3-Aminobenzanthrone and Their Reduced Analogues: Synthesis, Properties and Spectroscopy. *Molecules* **2021**, *26*.
11. Shaalan, N.; Mahdi, S. Synthesis, Characterization and Biological Activity Study of Some New Metal Complexes with Schiff's Bases Derived from [o-Vanillin] with [2-Amino-5-(2-Hydroxy-Phenyl)-1,3,4-Thiadiazole]. *Egypt. J. Chem.* **2021**, *64*, 4059–4067, doi:10.21608/ejchem.2021.66235.3432.
12. Subburu 1, M. e. al. Photooxidation of 2,2'-(Ethyne-1,2-Diyl)Dianilines: An Enhanced Photocatalytic Properties of New Salophen-Based Zn(II) Complexes. *Photochem* **2022**, *2*, 358–375.
13. Yan, L.; Zhang, S.; Xie, Y.; Lei, C. A Fluorescent Probe for Gallium(III) Ions Based on 2-Hydroxy-1-Naphthaldehyde and L-Serine. *Dye. Pigment.* **2020**, *175*, 108190, doi:10.1016/j.dyepig.2020.108190.
14. Zoubi, W. Al Biological Activities of Schiff Bases and Their Complexes: A Review of Recent Works. *Int. J. Org. Chem.* **2013**, *03*, 73–95, doi:10.4236/ijoc.2013.33a008.
15. Subburu 1, M. e. al. Photooxidation of 2,2'-(Ethyne-1,2-Diyl)Dianilines: An Enhanced Photocatalytic Properties of New Salophen-Based Zn(II) Complexes. *Photochem* **2022**, *2*, 358–375.17 16.
16. Zoubi, W. Al Biological Activities of Schiff Bases and Their Complexes: A Review of Recent Works. *Int. J. Org. Chem.* **2013**, *03*, 73–95, doi:10.4236/ijoc.2013.33a008.
17. Aly, S.A.; Fathalla, S.K. Preparation, Characterization of Some Transition Metal Complexes of Hydrazone Derivatives and Their Antibacterial and Antioxidant Activities. *Arab. J. Chem.* **2020**, *13*, 3735–3750, doi:10.1016/j.arabjc.2019.12.003.

18.Majeed, N. Eco-Friendly and Efficient Composition, Diagnosis Theoretical, Kinetic Studies, Antibacterial and Anticancer Activities of Mixed Some Metal Complexes of Tridentate Schiff Base Ligand. *Int. J. Pharm. Res.* **2021**, *13*, doi:10.31838/ijpr/2021.13.01.428.